Brain structure-function coupling is unique to individuals across multiple frequency bands: a graph signal processing study

Alessandra Griffa
Institute of Bioengineering, Center of Neuroprosthetics, Ecole Polytechnique Fédérale de Lausanne (EPFL),
Department of Radiology and Medical Informatics, University of Geneva (UNIGE),
Leenaards Memory Centre, Lausanne University Hospital and University of Lausanne.
Geneva, Switzerland
alessandra.griffa@epfl.ch

Maria Giulia Preti
Institute of Bioengineering, Center of Neuroprosthetics, Ecole Polytechnique Fédérale de Lausanne (EPFL),
Department of Radiology and Medical Informatics, University of Geneva (UNIGE),
CIBM Center for Biomedical Imaging.
Geneva, Switzerland
maria.preti@epfl.ch

***Abstract*— The relation between brain functional activity and the underlying structure is complex and varies depending on the specific brain region. Recently, we used graph signal processing to introduce the structural-decoupling index (SDI), a novel metric quantifying structure-function coupling in brain regions, based on graph spectral filtering of functional activity. At slow temporal scales accessible with resting-state functional magnetic resonance imaging, the SDI showed a meaningful spatial gradient from unimodal (more coupled) to transmodal regions (more liberal). It also showed to perform very well for brain fingerprinting; i.e., individuals could be classified with near perfect accuracy based on their SDI. Here, we investigate structure-function coupling at faster temporal scales and its specificity to individuals, by means of resting-state magnetoencephalography (MEG) of 84 healthy subjects. We found that the MEG SDI forms a cortical gradient from task-positive regions, more coupled, to task-negative regions, highly decoupled. Great specificity of the SDI to individuals was confirmed, with largest subject classification accuracies in the beta and alpha bands. We conclude that structure-function coupling changes across temporal scales of investigation and provides rich signatures of individual brain organization at rest.**

Keywords — graph signal processing, fingerprinting, MEG, structural-decoupling index, brain.

I. INTRODUCTION

The relation between brain functional activity and structural architecture remains to date an open question in neuroscience. In previous studies, we introduced the structural decoupling index (SDI), a regional measure defined within a graph signal processing (GSP) framework [1] that quantifies the degree of structure-function coupling for each brain region [2]. In this context, the structural connectome obtained from diffusion-weighted magnetic resonance imaging (MRI) serves as graph, and functional activity patterns defined at the same nodes (brain regions) as graph signals. During resting-state and at slow temporal scale probed with functional MRI (0.01-0.15 Hz), the SDI shows a very specific spatial distribution, spanning from lower-order sensory and somatomotor functional areas, with function highly aligned to the structure underneath, to higher-order fronto-parietal ones, more independent from the structure [2]. At this slow temporal scale, functional connectivity components *decoupled* from the underlying structure demonstrate high specificity to individuals and explain a significant portion of inter-individual cognitive variability, at a level that exceeds connectivity components coupled with structure [3]. At faster temporal scales accessible with electrophysiological recordings (1-50 Hz), the brain activity signal can be compactly represented as a linear combination of structural connectome harmonics [4] which concentrate in the lower frequencies of the connectome spectrum [5]. However, the spatial distribution of regional structure-function coupling across fast temporal scales and their fingerprinting value have not yet been investigated. Here, we study for the first time how brain structure-function dependencies change across temporal scales probed with resting-state magnetoencephalography (MEG) and how they relate to individual subjects. To this aim, we assess the spatial distribution and subject classification performance of the SDI computed across distinct (temporal) frequency bands −delta, theta, alpha, beta, gamma−, thus evaluating the fingerprinting values of such GSP-derived measure across fast temporal scales. In fact, functional brain activity is known already for the ability to well distinguish between individuals [6–8]. MEG functional connectivity profiles were shown to identify a subject within a large group (fingerprinting), particularly when considering the alpha and beta

frequency bands, and with main contributions from parieto-occipital regions including parts of the default mode, frontoparietal, and dorsal attention networks [7]. In parallel, brain structural features have also been used in the past for brain fingerprinting [9]. However, these features analyze either structure or function alone: we aim here to fill this gap by characterizing the properties and fingerprinting value of structure-function dependency profiles at fast temporal scales.

II. Methods

A. MEG cohort

The data used for this study consisted of structural (T1-weighted MRI) and functional (resting-state MEG) acquisitions from $N_s = 84$ subjects (29.0 ± 3.6 years, 46% women) of the 1200 Subjects release of the Human Connectome Project (HCP-MEG) [10]. T1-weighted volumes were acquired at Washington University on a dedicated Siemens 3T Skyra scanner with a 32-channel head coil, with 0.7 mm isotropic voxel size. MEG recordings were collected at St. Louis University on a whole-head MAGNES-3600 system including 248 magnetometers and 23 reference channels, at 2034 Hz sampling rate and in three separate runs of approximately 6 min each within a single-day. Only the first two runs were considered in this study and randomly tagged as test and retest datasets for each subject. Complete details about MRI and MEG data can be found elsewhere [10,11].

B. Data Processing

T1-weighted volumes were segmented into 148 cortical regions of interest (Destrieux parcellation [12]) within the HCP pipeline. Preprocessed sensor-level MEG data were downloaded from the HCP database and projected to the 148 region centroids to obtain source-level MEG timecourses. The HCP preprocessing includes rejection of bad channels and data segments; notch filtering to remove power line noise; artefact removal using independent component analysis; temporal downsampling to 500 Hz [13]. The same processing procedure explained in details in [7] and briefly outlined in the following was adopted here. Source reconstruction was performed with FieldTrip and linearly constrained minimum-variance beamforming method using subject-specific forward lead field models [14]. The source timecourses of each subject and run were then subdivided into 19 epochs of 12 s duration (6108 samples) and bandpass filtered into the five canonical frequency bands: delta (1–4 Hz), theta (4–8 Hz), alpha (8–13 Hz), beta (13–30 Hz), and gamma (30–48 Hz) using two-way FIR filters of order 2034. The envelope of band-passed timecourses was computed as the magnitude of the Hilbert transform [13] of signals and used for the following GSP analyses. Finally, a

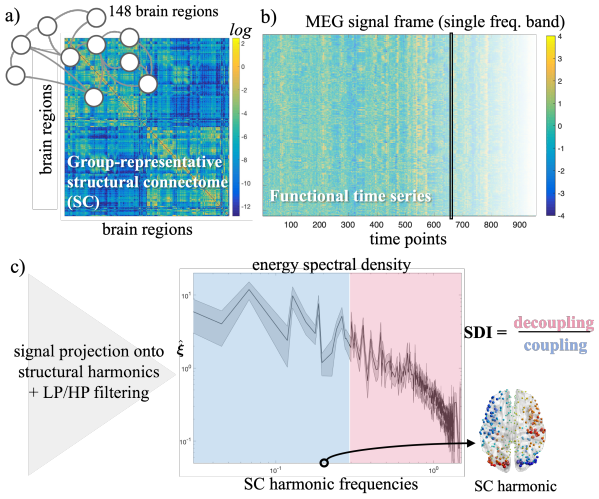

Fig.1 Graph Signal Processing Pipeline. a) A group representative healthy structural connectome (SC) is obtained by averaging the SCs of 100 HCP subjects based on the Destrieux 148-regions parcellation. b) For each subject and run, single frequency band magnetoencephalography (MEG) functional data at each timepoint was projected onto SC harmonics (SC Laplacian eigenvectors) and c) filtered with a low-pass (LP) and high-pass (HP) filter, with cutoff chosen based on median energy split criterium. The SDI was computed as the ratio between the decoupled and coupled portions of signals.

reference structural connectome was computed from the diffusion MRI data of 100 HCP subjects (U100 release) as previously described in [3], representing the weighted white-matter connections between the same 148 cortical regions considered for functional processing.

C. GSP Framework and Structural-Decoupling Index

The GSP framework detailed in [2] and summarized in Fig. 1 was used to obtain the SDI for each subject, run, and frequency band. In particular, the reference structural connectome is considered as adjacency matrix of a graph and symmetrically normalised with respect to the degree matrix to obtain A_{symm}. Structural harmonics u_k are then obtained by eigendecomposition of the structural Laplacian $L = I - A_{symm}$ (where I is the identity matrix):

$$LU = U\Lambda\,, \qquad (1)$$

where each eigenvalue $[\Lambda_{k,k}] = \lambda_k$ can be interpreted as spatial frequency of the corresponding structural harmonic (eigenvector) u_k. Functional data s_t at each timepoint t is then projected onto the structural harmonics by assessing the spectral coefficients

$$\hat{s_t} = U^T s_t\,, \qquad (2)$$

and filtered into two components with ideal low- and high-pass filters; i.e., a coupled one obtained as $s_t^C = U^{(low)}\widehat{s_t}$ and a decoupled one as $s_t^D = U^{(high)}\widehat{s_t}$, respectively ($U^{(low)}$ being a matrix with the first eigenvectors complemented by zeros, and $U^{(high)}$ being a matrix with first columns of zeros followed by the remaining last eigenvectors). To avoid subject-bias, the cut-off to filter functional activity based on structural harmonics was fixed to the average spectral median-split value across subjects, epochs and runs, for each frequency band, and this corresponded to $c = 56, 56, 58, 56, 55$ for the delta, theta, alpha, beta and gamma frequency bands, respectively. Coupling N^C and decoupling N^D were quantified for each epoch and brain region as the *l2*-norm across time of the coupled and decoupled signal portions s_t^C and s_t^D, and the SDI was computed as their ratio:

$$\text{SDI} = N^D \ / \ N^C. \qquad (3)$$

The SDI cortical map of each subject, run (test/retest), and frequency band was obtained as the average over the 19 epochs.

D. Subject Classification

Linear support vector machine (SVM) classifiers with $N_s = 84$ classes were trained to identify individuals based on their structure-function coupling characteristics in different frequency bands (each band was analysed independently). Subject classification accuracy was assessed with 7-fold cross-validation (CV), where each time the SVM was trained on 156 data points (i.e., 72-subject test and retest datasets, and 12-subject retest dataset) and tested on unseen 12 data points (i.e., 12-subject test dataset). In each CV loop, a *one-versus-all* multiclass linear SVM classifier with error-correcting output codes modelling was trained on training data with the *fitcecoc* MATLAB v.R2019b function and used to predict the subject in the unseen data. No hyperparameter tuning was involved in the classifiers' training. This procedure was repeated 100 times to obtain classification accuracy confidence intervals.

E. Brain Fingerprinting Patterns

Analyses of variance (ANOVAs) were performed to identify brain patterns reflecting the main effect of *subject,* therefore including regions where SDI is more specific to individuals (which we can also refer to as *fingerprinting patterns*) [3]. Regional SDI values in a specific frequency band were used as dependent variable, and subject as explanatory variable. F-values were considered significant for $p < .05$, Bonferroni

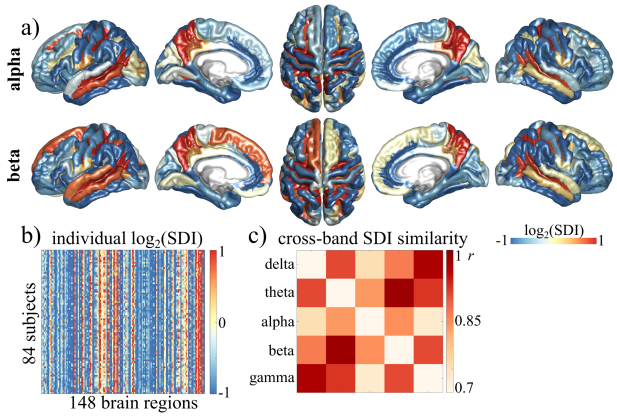

Fig.2 MEG structural-decoupling index (SDI). a) Group-average SDI cortical distributions in the alpha (first row) and beta (second row) bands, with red tones highlighting regions more coupled with the structure underneath, and blue tones indicating regions more decoupled from structure (log2 scaling). b) Alpha-band SDI values for individual subjects (test data) across brain regions (log2 scaling). c) Similarity between SDI cortical distributions across frequency bands, quantified with the Pearson's correlation coefficient (*r*).

corrected across brain regions. The analysis was repeated for each frequency band.

III. Results

A. Structure-Function Coupling across Frequency Bands

The regional SDI was computed for each subject (test and retest data) and each frequency band. The cortical distributions of SDI values were highly similar across subjects, for all frequency bands (average inter-subject correlation $r = 0.903 \pm 0.058$) (Fig. 2b). Fig. 2a depicts the group-average cortical SDI distribution in the alpha and beta bands. A clear dichotomous pattern is visible: on one side, task-positive networks including somatomotor, visual, and frontoparietal regions are coupled with the underlying structural graph (blue regions). On the other side, task-negative (default mode) networks are more decoupled from structure (red regions). The structures with higher SDI values (stronger decoupling) were the bilateral precuneus, posterior cingulate, and middle temporal cortices in all the investigated bands. The SDI cortical patterns were relatively similar across frequency bands (Fig. 2c; average cross-band SDI correlation $r = 0.872$). The largest similarities were found between the delta and gamma bands ($r = 0.966$) and the theta and beta bands ($r = 0.979$); the SDI pattern in the alpha bands was the most distinct (average $r = 0.794$).

B. Subject Classification

Subject identification accuracy assessed with SVM

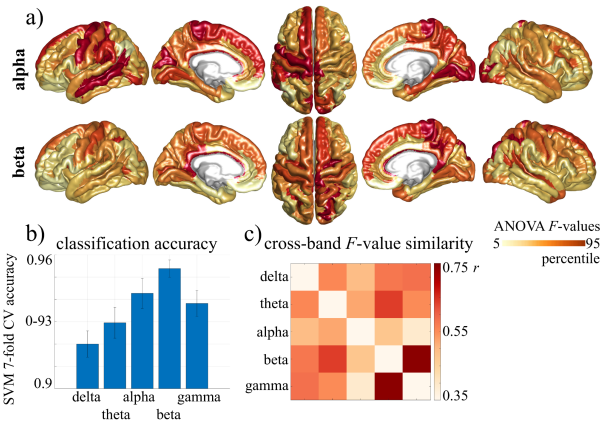

Fig.3 SDI fingerprinting at fast temporal scales. a) Cortical fingerprinting patterns (F-values from ANOVA analyses) in the alpha (first row) and beta (second row) bands. b) Subject classification accuracies in the five frequency bands. Bars and error whiskers indicate mean ± standard deviation across 100 runs of 7-fold cross-validation. c) Similarity between fingerprinting cortical patterns across frequency bands, quantified with the Pearson's correlation coefficient (r).

classification and repeated 7-fold CV was largely above chance level, ranging from 92.00% in the delta band to 95.38% in the beta band. Identification accuracy was higher in the beta and alpha (94.27%) bands, followed by the gamma (93.82%), theta (92.95), and delta bands, with low variability across CV runs (accuracy standard deviation across frequency bands ranged between 0.39% and 0.69%) (Fig. 3b).

C. *Brain Fingerprinting Patterns*

Brain regional contribution to subject identification was assessed with ANOVA analyses, separately for each frequency band. Almost all brain regions significantly contributed to subject identification (delta: 98%, theta: 98%, alpha: 99%, beta: 100%, gamma: 99% significant brain regions, i.e., $p < .05$ corrected for multiple comparisons due to the 148 brain regions). Overall, the cortical fingerprinting patterns mainly concentrate in the superior frontal gyri, posterior cingulate cortices/precuneus, middle temporal gyri (part of the default mode network) and secondary visual cortices, including both regions coupled and decoupled from structure (compare Fig. 2a and Fig. 3a).
Yet, there were significant variations across frequency bands, with average cross-band similarity of fingerprinting patterns $r = 0.554 \pm 0.093$ (Fig. 3c).

IV. Discussion

In this work, we investigated cortical patterns of structure-function coupling in 84 healthy subjects, in relation to five different frequency bands and to subject identification accuracy (brain fingerprinting). We found that, at the fast temporal scales accessible with MEG, the group-average SDI cortical patterns are remarkably different from those observed at slower temporal scales. Functional-MRI SDI mainly evolves along a lower-order to higher-order system axis, with visual and somatomotor regions coupled with structure and fronto-parietal regions for higher-order cognition decoupled from structure [2]. Instead, in MEG data the SDI seems to vary along a task-positive to task-negative axis, with default mode network regions distinctively decoupled from structure. Yet, the functional activity of regions of the fronto-parietal network appears coupled with the underlying structural graph. Future work should directly compare SDI topographies derived from fMRI and MEG data recorded in the same subjects, and explore how they may differ as a function of the temporal and spatial (parcellation) scales of investigation.
Further, we confirmed the high fingerprinting value of SDI, even at these faster temporal scales, and found that the subject uniqueness of MEG SDI fingerprints is higher in the beta and alpha bands. This result is in line with previous fingerprinting analyses on MEG functional connectivity which however discard the structural connectivity information [7,15]. Similarly to SDI, subject classification accuracy based on MEG functional connectivity is particularly high in the alpha and beta bands (84% to 99% [7,15]), even though accuracies vary depending on the way functional connectivity is quantified (particularly, phase-based vs amplitude-based connectivity measures), with spatial leakage effects representing a potential confounding factor [7]. Future work should investigate the value of jointly considering multiple frequency bands, and/or multiple tasks [16] for MEG-based SDI assessment and individual fingerprinting.

Finally, this preliminary work may be extended by investigating the relationship between individual SDI patterns across different frequency bands, and individual cognitive and behavioral profiles.

V. Conclusion

The level of structure-function coupling in different brain regions and its specificity to individual subjects depend on the temporal scales of investigation. The structural-decoupling index provides a new signature of brain organization at the fast temporal scales accessible with MEG.

Acknowledgment

Data were provided by the Human Connectome Project, WU-Minn Consortium (Principal Investigators: David Van Essen and Kamil Ugurbil; 1U54MH091657) funded by the 16 NIH Institutes and Centers that support

the NIH Blueprint for Neuroscience Research; and by the McDonnell Center for Systems Neuroscience at Washington University. M. G. P. was supported by the CIBM Center for Biomedical Imaging, a Swiss research center of excellence founded and supported by Lausanne University Hospital (CHUV), University of Lausanne (UNIL), Ecole Polytechnique Fédérale de Lausanne (EPFL), University of Geneva (UNIGE) and Geneva University Hospitals (HUG). AG was supported by the Swiss National Science Foundation (grant number 320030_173153).

REFERENCES

[1] D.I. Shuman, S.K. Narang, P. Frossard, A. Ortega, P. Vandergheynst, "The emerging field of signal processing on graphs: Extending high-dimensional data analysis to networks and other irregular domains," IEEE Signal Processing Magazine, vol. 30, pp. 83–98, 2013. https://doi.org/10.1109/MSP.2012.2235192.

[2] M.G. Preti, D. Van De Ville, "Decoupling of brain function from structure reveals regional behavioral specialization in humans," Nature Communications, vol. 10, pp. 4747, 2019. https://doi.org/10.1038/s41467-019-12765-7.

[3] A. Griffa, E. Amico, R. Liégeois, D.V.D. Ville, M.G. Preti, "Brain structure-function coupling provides signatures for task decoding and individual fingerprinting," NeuroImage, vol. 118970, 2022. https://doi.org/10.1016/j.neuroimage.2022.118970.

[4] J. Rué-Queralt, K. Glomb, D. Pascucci, S. Tourbier, M. Carboni, S. Vulliémoz, G. Plomp, P. Hagmann, "The connectome spectrum as a canonical basis for a sparse representation of fast brain activity," NeuroImage, vol. 244, pp. 118611, 2021. https://doi.org/10.1016/j.neuroimage.2021.118611.

[5] K. Glomb, J. Rué Queralt, D. Pascucci, M. Defferrard, S. Tourbier, M. Carboni, M. Rubega, S. Vulliémoz, G. Plomp, P. Hagmann, "Connectome spectral analysis to track EEG task dynamics on a subsecond scale," NeuroImage, vol. 221, pp. 117137, 2020. https://doi.org/10.1016/j.neuroimage.2020.117137.

[6] E.S. Finn, X. Shen, D. Scheinost, M.D. Rosenberg, J. Huang, M.M. Chun, X. Papademetris, R.T. Constable, "Functional connectome fingerprinting: identifying individuals using patterns of brain connectivity," Nature Neuroscience, vol. 18, pp. 1664–1671, 2015. https://doi.org/10.1038/nn.4135.

[7] E. Sareen, S. Zahar, D.V.D. Ville, A. Gupta, A. Griffa, E. Amico, "Exploring MEG brain fingerprints: Evaluation, pitfalls, and interpretations," NeuroImage, vol. 240, pp. 118331, 2021. https://doi.org/10.1016/j.neuroimage.2021.118331.

[8] M. Demuru, A.A. Gouw, A. Hillebrand, C.J. Stam, B.W. van Dijk, P. Scheltens, B.M. Tijms, E. Konijnenberg, M. ten Kate, A. den Braber, D.J.A. Smit, D.I. Boomsma, P.J. Visser, "Functional and effective whole brain connectivity using magnetoencephalography to identify monozygotic twin pairs," Sci Rep. 240 (2021) vol. 7, pp. 1–11, 2017. https://doi.org/10.1038/s41598-017-10235-y.

[9] S. Mansour L, Y. Tian, B.T.T. Yeo, V. Cropley, A. Zalesky, "High-resolution connectomic fingerprints: Mapping neural identity and behavior," NeuroImage, vol. 229, pp. 117695, 2021. https://doi.org/10.1016/j.neuroimage.2020.117695.

[10] L.J. Larson-Prior, R. Oostenveld, S. Della Penna, G. Michalareas, F. Prior, A. Babajani-Feremi, J.-M. Schoffelen, L. Marzetti, F. de Pasquale, F. Di Pompeo, J. Stout, M. Woolrich, Q. Luo, R. Bucholz, P. Fries, V. Pizzella, G.L. Romani, M. Corbetta, A.Z. Snyder, "Adding dynamics to the Human Connectome Project with MEG," NeuroImage, vol. 80, pp. 190–201, 2013. https://doi.org/10.1016/j.neuroimage.2013.05.056.

[11] D.C. Van Essen, S.M. Smith, D.M. Barch, T.E.J. Behrens, E. Yacoub, K. Ugurbil, "The WU-Minn Human Connectome Project: An overview," NeuroImage, vol. 80, pp. 62–79, 2013.

[12] C. Destrieux, B. Fischl, A. Dale, & E. Halgren, "Automatic parcellation of human cortical gyri and sulci using standard anatomical nomenclature," NeuroImage, vol. 53, no. 1, pp. 1–15, 2010.

[13] J.M. Brookes, J.R. Hale, J.M. Zumer, C.M. Stevenson, S.T. Francis, G.R. Barnes, J.P. Owen, P.G. Morris, S.S. Nagarajan, "Measuring functional connectivity using MEG: Methodology and comparison with fcMRI," NeuroImage, vol. 56, no. 3, pp. 1082-1104, 2011.

[14] R. Oostenveld, P. Fries, E. Maris, J.M. Schoffelen, "FieldTrip: Open source software for advanced analysis of MEG, EEG, and invasive electrophysiological data," Comput Intell Neurosci., vol. 2011, pp. 156869. 2011, doi: 10.1155/2011/156869.

[15] J. da Silva Castanheira, H.D. Orozco Perez, B. Misic, S. Baillet, "Brief segments of neurophysiological activity enable individual differentiation," Nat Commun., vol. 12, pp. 5713, 2021. https://doi.org/10.1038/s41467-021-25895-8.

[16] Maximilian Nentwich, Lei Ai, Jens Madsen, Qawi K. Telesford, Stefan Haufe, Michael P. Milham, Lucas C. Parra, "Functional connectivity of EEG is subject-specific, associated with phenotype, and different from fMRI," NeuroImage, vol. 218, pp. 117001, 2020. https://doi.org/10.1016/j.neuroimage.2020.117001.